J|A|C|S ARTICLES

Published on Web 10/02/2009

Synthesis of a Nitrogen-Stabilized Hexagonal Re_3ZnN_x Phase Using High Pressures and Temperatures

George Serghiou,*,† Christophe L. Guillaume,†,¶ Andrew Thomson,†,⊥ Jean-Paul Morniroli,‡ and Dan J. Frost§

University of Edinburgh, School of Engineering and Centre for Materials Science, Kings Buildings, Mayfield Road, EH9 3JL U.K., Laboratoire de Métallurgie Physique et Génie des Matériaux, UMR CNRS 8517, Université des Sciences et Technologies de Lille et Ecole Nationale Supérieure de Chimie de Lille, Cité Scientifique, 59655 Villeneuve d'Ascq Cedex, France, and Bayerisches Geoinstitut, Universität Bayreuth, D-95440, Bayreuth, Germany

Received May 15, 2009; E-mail: george.serghiou@ed.ac.uk

Abstract: High pressure can induce profound changes in solids. A significant barrier to new alloys and ceramics, however, is that targeted starting materials may not react with each other, even with the help of pressure. We use nitrogen, in a new capacity, to incorporate two otherwise unreactive elements, Re and Zn, in the same structure when pressure alone does not suffice, without nitrogen altering the resulting backbone structure. Synthesis experiments up to 20 GPa and 1800 K show that while no Re−Zn alloy or solid solution is formed, a novel Re_3ZnN_x ordered solid solution is formed, at 20 GPa, with nitrogen occupying Re-coordinated cages. We put forth that unlike pure Re_3Zn, our novel hexagonal Re_3ZnN_x structure is stabilized by nitrogen bond formation with rhenium. Pressure lifts the pronounced ambient Zn anisotropy, making it more compatible with Re and likely facilitating incorporation of the structure-stabilizing nitrogen anion. This methodology and result denote further options for removing impasses to material preparation, thus opening new avenues for synthesis. These can also be pursued with other ions including carbon, hydrogen, and oxygen, in addition to nitrogen.

Introduction

The use of high pressures is drastically enhancing the range of known materials. In the nascent nitride landscape, principal novel architectures prepared are the cubic spinel structure for group IVA systems,[1−3] the thorium phosphide structure for group IVB systems,[4] ordered hexagonal molybdenum nitride,[5] polymerized single bonded nitrogen,[6] and noble nitrides containing single bonded dinitrogen units.[7] The emerging landscape already contains several important properties ranging from high hardness to tunable band-gaps, that will clearly be enriched further. We are using nitrogen here, however, in a different way, to increase the options and range of what we can make. In the nitrides described above, nitrogen is a network participant. We use nitrogen here to facilitate reaction between unreactive elements to form novel alloys that cannot be made at ambient pressure, or with high pressure alone. While nitrogen is in the structure to stabilize it, it does not change the structural architecture. We focus here on Re and Zn. Existing rhenium alloys exhibit superconductivity and are used as catalysts and as engine parts in jets. Zinc is a primary component of brass and is alloyed with iron to prevent corrosion. Fundamentally, both rhenium and zinc are hexagonal close packed. Rhenium has a normal c/a lattice constant ratio of 1.61 which remains normal to over 2 million atmospheres.[8] Zinc on the other hand is highly anisotropic, with a c/a ratio of 1.86 which becomes more normal upon compression, reaching a value of about 1.67 at 20 GPa.[9] Indeed Zn is the focus of intense interest[10] in correlating how the underlying electronic structure transforms with the change in anisotropy. Here, based on a detailed analysis, presented in this paper, we use in summary a simple two-step design principle to prepare a novel Re−Zn solid solution. We employ pressure to make Zn more compatible with Re with respect to an ordered solid solution formation and then add a small amount of nitrogen to make the ordered solid solution favorable.

Results and Discussion

Our Re−Zn mixtures (see Methods for experimental procedures) heated at ambient pressure confirm that no reaction takes

† University of Edinburgh.
‡ University of Lille.
§ University of Bayreuth.
¶ Present address: School of Physics, University of Edinburgh, U.K.
⊥ Present address: BP Chemicals Ltd., Hull, U.K.

(1) Serghiou, G.; Miehe, G.; Tschauner, O.; Zerr, A.; Boehler, R. *J. Chem. Phys.* **1999**, *111*, 4659–4662.
(2) Zerr, A.; Miehe, G.; Serghiou, G.; Schwarz, M.; Kroke, E.; Riedel, R.; Fuess, H.; Kroll, P.; Boehler, R. *Nature* **1999**, *400*, 340–342.
(3) Scotti, N.; Kockelmann, W.; Senker, J.; Trassel, S.; Jacobs, H. *Z. Anorg. Allg. Chem.* **1999**, *625*, 1435–1439.
(4) Zerr, A.; Miehe, G.; Riedel, R. *Nat. Mater.* **2003**, *2*, 185–189.
(5) Bull, C. L.; McMillan, P. F.; Soignard, E.; Leinenweber, K. *J. Solid State Chem.* **2004**, *177*, 1488–1492.
(6) Eremets, M. I.; Gavriliuk, A. G.; Trojan, I. A.; Dzivenko, D. A.; Boehler, R. *Nat. Mater.* **2004**, *3*, 558–563.
(7) Crowhurst, J. C.; Goncharov, A. F.; Sadigh, B.; Evans, C. L.; Morall, P. G.; Ferreira, J. L.; Nelson, A. J. *Science* **2006**, *311*, 1275–1278.
(8) Vohra, Y. K.; Duclos, J.; Ruoff, A. L. *Phys. Rev. B* **1987**, *36*, 9790–9792.
(9) Kenichi, T.; Hiroshi, Y.; Hiroshi, F.; Takumi, K. *Phys. Rev. B* **2002**, *65*, 132107–13110.
(10) Gaston, N.; Paulus, B.; Wedig, U.; Jansen, M. *Phys. Rev. Lett.* **2008**, *100*, 226404–226408.

 10.1021/ja903976j CCC: $40.75

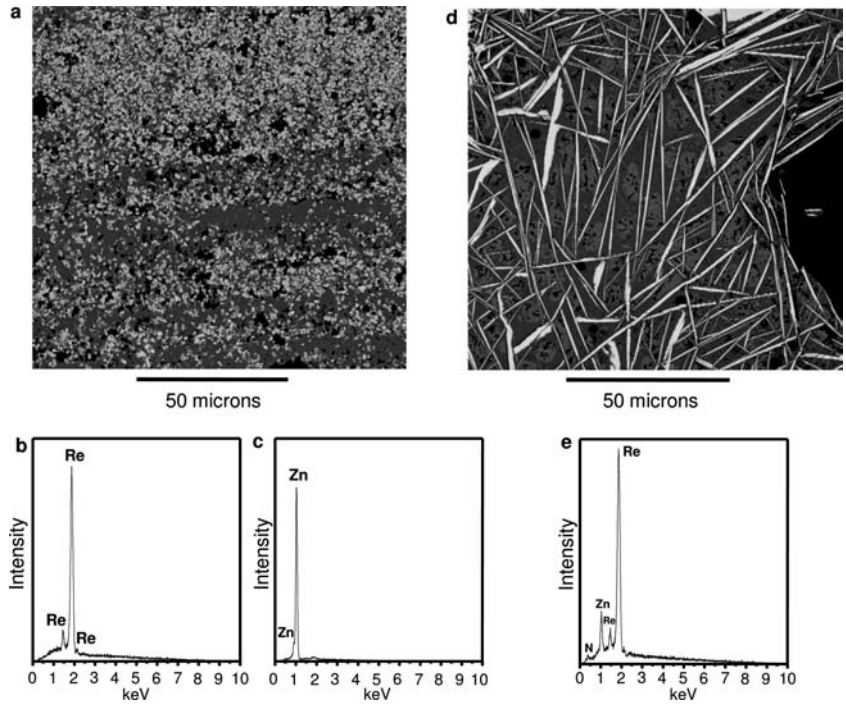

Figure 1. Images and chemical analysis of Re and Zn recovered from 20 GPa and 1800 K. (a) SEM image in BSE mode of a polished section after heating Re with Zn at 1800 K at 20 GPa for 2 min followed by temperature and then pressure quenching. (b, c) Semiquantitative results from numerous EDX analyses of the recovered sample reveal no reaction and virtually complete segregation of Re (light contrast regions), from Zn (dark contrast regions). The black regions in image a are epoxy and holes. (d) SEM images in BSE mode of a polished section after heating Re with Zn_3N_2 at 20 GPa followed by temperature and then pressure quenching. (e) Semiquantitative EDX analyses show that the lighter contrast regions exhibit a Re_3ZnN_x stoichiometry. The nitrogen content is small, requiring the present 10 kV acceleration voltage to enhance its detection. The crystals likely contain less than $x = 0.5$. The darker contrast regions contain zinc, zinc oxynitride, and a sparser zinc nitride presence.

place between the two components,[11] and similarly we find that no reaction takes places between Re and Zn_3N_2 heated either at ambient pressure or at 5 GPa. The recovered sample after heating the Re−Zn mixture at 1800 K at 20 GPa also shows no reaction between the two (Figure 1a−c). The situation is drastically different for the case of the recovered sample after heating Re together with Zn_3N_2 at 1800 K at 20 GPa (Figure 2d,e). All the light contrast regions within the capsule are homogeneous, containing Re, Zn, and N with a semiquantitative stoichiometry given by energy dispersive X-ray analysis of Re_3ZnN_x.

To investigate the structure, numerous selected-area and microdiffraction patterns were collected from single crystallites using up to 30° and 60° tilt angles in two mutually perpendicular directions. Tilting was essential because individual crystallites were thin and distributed themselves preferentially along one crystallographic plane. That is, virtually regardless of beam-size or beam location the same zone axis diffraction pattern (Figure 2a) or distorted variations of it were obtained from the sample. This zone axis diffraction pattern (Figure 2a) and its particular intensity distribution together with its characteristic superlattice reflections are a signature of the [001] basal plane of both the $D0_{19}$ structure (Ni_3Sn type) and its longer period $D0_{24}$ modification (Ni_3Ti type)[12] (Figure 2b). By correlating measured diffraction patterns at different tilt angles with simulated diffraction patterns at those tilt angles for a specified sample thickness, we were able to identify the correct assign-

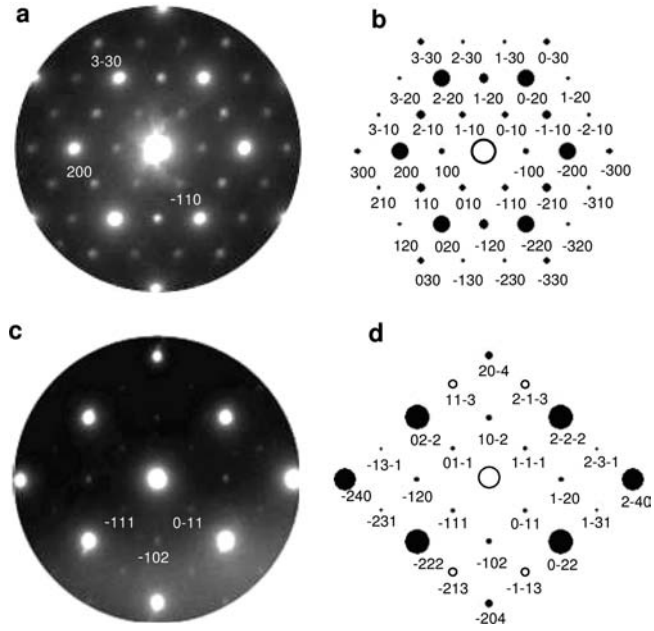

Figure 2. Zone-axis microdiffraction patterns[15] of Re_3ZnN_x. (a, b) Experimental and simulated [001] zone-axis diffraction patterns of the $D0_{24}$ hexagonal Re_3ZnN_x superlattice structure. (c, d) Experimental and simulated [211] zone-axis diffraction patterns of the $D0_{24}$ hexagonal Re_3ZnN_x superlattice structure. Differentiating between the intimately related $D0_{19}$ and $D0_{24}$ modifications became evident from the presence of the ({−111}, {0−11}, {1−1−1}, {01−1}) reflections in the [211] zone-axis diffraction pattern, which are induced by a doubling of the $D0_{19}$ *c*-axis, giving rise, with the appropriate adjustment of the crystallographic coordinates, to the $D0_{24}$ structure.

(11) Massalski, T. *Binary Alloy Phase Diagrams*, 2nd ed.; ASM: Materials Park, OH, 1990; Vol. 2.
(12) Gasgnier, M.; Schiffmacher, G.; Caro, P. *J. Less-Common Metals* **1976**, *50*, 177–188.

Table 1. Atomic Coordinates for Re_3ZnN_x: [$D0_{24}$ structure type, space group $P6_3/mmc$, $a = 5.6$ Å, $c = 8.8$ Å, $Z = 4$]

atom	site	*x*	*y*	*z*
Re1	6g	1/2	0	0
Re2	6h	5/6	2/3	1/4
Zn1	2a	0	0	0
Zn2	2c	1/3	2/3	1/4
N1	4f	1/3	2/3	7/8

ment as $D0_{24}$ (Ni_3Ti type)[13] (Figure 2c,d) and simultaneously eliminate further possibilities such as the cubic antiperovskite structure (Cu_3Au type). The space group of the $D0_{24}$ type is $P6_3/mmc$ and the lattice parameters showed a good fit to $a = 5.6$ Å and $c = 8.8$ Å.[14,15] The foil-like nature of the crystals is apparently facilitated by enhanced growth along the basal plane as compared to the *c*-axis direction. Preferred orientation along the [001] zone in $D0_{24}$ crystals appears to be favored, as it has already been reported in the original discovery of the prototype (Ni_3Ti) structure type.[13] A table with atomic coordinates and a schematic representation of the novel hexagonal Re_3ZnN_x nitride are shown in Table 1 and Figure 3.

On the basis of these measurements, a $D0_{24}$ structure with Re_3ZnN_x composition is recovered after heating Re and Zn_3N_2 at 1800 K at 20 GPa, while Re and Zn under the same conditions do not form an alloy. We consider here in greater detail both polyhedral and atomic packing descriptions of $D0_{24}$, closely related $D0_{19}$, and the antiperovskite phase,[16] because the two descriptions provide complementary insight into why a Re−Zn superlattice structure is formed and why nitrogen is required to stabilize it. Concomitantly, greater detail is provided into the crystal structure assignment, the nitrogen site-occupancy, and the novelty of the $D0_{24}$ structure.

Polyhedral Analysis. The archetypical $D0_{24}$ A_3B structure has four formula units in the unit cell.[13] There are several examples of this structure that can be prepared at ambient pressure, the prototype structure being Ni_3Ti. The cell is composed of four empty octahedra which are all linked to each other by corners and faces and whose vertices are occupied exclusively by A atoms. They propagate in a zigzag fashion along the *c*-axis. The unit cell also contains seven empty tetrahedra which are connected to each other and to the octahedra by corners and edges. Three of the tetrahedra have three A atoms and one B atom occupying their vertices, and the other four each have two A atoms and two B atoms occupying their vertices. The archetypical A_3B $D0_{19}$ structure[17] of which there are many examples that can be prepared at ambient pressure, such as Ti_3Al, Ni_3Sn, or Mg_3Cd, is composed of two types of empty octahedra. One has only A atoms at the six vertices [A_6] and the other has four A atoms and two B atoms at its vertices [A_4B_2]. The [A_6] units form face-sharing columns along the *c*-axis as do the [A_4B_2] units, and the two types of units share edges in the basal plane, but there is no connectivity between like octahedra in this plane. The antiperovskite structure (Cu_3Au)[18] is composed of corner-sharing empty octahedra, the vertices of which are exclusively occupied by A atoms, and dodecahedra, which are centered by A atoms, with B atoms exclusively on the twelve vertices of the dodecahedra.

Several previous ambient pressure studies on the cubic antiperovskite structures reveal that smaller ions including hydrogen, deuterium, carbon, and nitrogen ions are all incorporated interstitially in the octahedral interstitial position.[19−29] Prior to this work, for the $D0_{19}$ and $D0_{24}$ hexagonal modifications, the only reports, to our knowledge, of interstitial ions entering the structures were hydrogen for both modifications and deuterium for $D0_{19}$.[28−30] In all the above cases, invariably, the ions enter the octahedral site with the vertices occupied solely by the transition-metal ions. $D0_{24}$ contains octahedral sites, coordinated solely by Re. Further, the tetrahedral sites are too small to incorporate nitrogen. On the basis of these considerations, nitrogen in the present case is also, placed interstitially in the pure Re octahedra. For the case of the $D0_{19}$ structure, increasing the hydrogen or deuterium content ultimately causes a phase transition to the Cu_3Au cubic antiperovskite modification.[28,29] For the case of nitrogen, attempts to incorporate it into an existing $D0_{19}$ structure resulted in the Cu_3Au structure,[20,26] that is, there was no stability field for a nitrogen-containing hexagonal super-

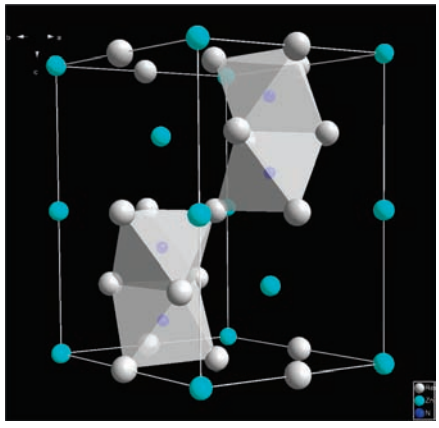

Figure 3. Schematic of the Re_3ZnN_x structure. The hexagonal $P6_3/mmc$ $D0_{24}$ Re_3ZnN_x structure contains octahedra which are all linked to each other, by corners and faces and whose vertices are occupied exclusively by Re atoms. They propagate in a zigzag fashion along the *c*-axis. The unit cell also contains seven tetrahedra (not drawn in) which are discussed further in the text. Nitrogen exclusively occupies the centers of Re octahedra. In the actual sample not all octahedra are likely filled. The Re atoms are colored light gray, the Zn atoms turquoise and the N atoms blue.

(13) Laves, F.; Wallbaum, H. J. *Z. Kristallogr.* **1939**, *101*, 78–93.
(14) Morniroli, J. P. Electron Diffraction 6.98, LMPGM UMR CNRS 8517, France, 2002.
(15) Morniroli, J. P. Electron Diffraction 7.01, LMPGM UMR CNRS 8517, France, 2004.
(16) Hume-Rothery, W.; Smallman, R. E.; Haworth, C. W. *The Structure of Metals and Alloys*, 5th ed.; The Chaucer Press: London, 1969.
(17) Rahlfs, P. *Metallwirtsch., Metallwiss., Metalltech.* **1937**, *16*, 343–345.
(18) Le Blanc, M.; Richter, K.; Schiebold, E. *Ann. Phys.* **1928**, *86*, 929–1005.
(19) Hutter, L. J.; Stadelmaier, H. H. *Z. Metallkd.* **1959**, *50*, 199–203.
(20) Xu, Y.; Elbicki, J. M.; Wallace, W. E.; Simizu, S.; Sankar, S. G. *IEEE Trans. Magn.* **1992**, *28*, 2569–2571.
(21) Stadelmaier, H. H.; Fraker, A. C. *Trans. Metall. Soc. AIME* **1960**, *218*, 571–572.
(22) Stadelmaier, H. H.; Fraker, A. C. *Z. Metallkd.* **1962**, *53*, 48–52.
(23) Vogtenhuber-Pawelczak, D.; Herzig, P. *J. Solid State Chem.* **1992**, *99*, 85–94.
(24) Ivanovskii, A. L.; Medvedeva, N. I.; Novikov, D. L. *Phys. Solid State* **1997**, *39*, 1035–1037.
(25) Schuster, J. C.; Bauer, J. *J. Solid State Chem.* **1984**, *53*, 260–265.
(26) Feng, W. J.; Li, D.; Ren, W. J.; Li, Y. B.; Li, W. F.; Li, J.; Zhang, Y. Q.; Zhang, Z. D. *J. Alloys Compd.* **2007**, *437*, 27–33.
(27) Vennstrom, M.; Andersson, Y. *J. Alloys Compd.* **2002**, *330−332*, 166–168.
(28) Vennstrom, M.; Grechnev, A.; Eriksson, O.; Andersson, Y. *J. Alloys Compd.* **2004**, *364*, 127–131.
(29) Grechnev, A.; Andersson, P. H.; Ahuja, R.; Eriksson, O.; Vennstrom, M.; Andersson, Y. *Phys. Rev. B* **2002**, *66*, 235104–235113.
(30) Ronnebro, E.; Noreus, D.; Gupta, M.; Kadir, K.; Hauback, B.; Lundqvist, P. *Mater. Res. Bull.* **2000**, *35*, 315–323.

lattice structure prior to this work. A second seminal difference from the previous cases involving hexagonal modifications is that reactions between the constituent elements making up the hexagonal modifications could occur with or without the presence of the interstitial additions, whereas in the present case, Re does not react with Zn either at ambient or at the highest pressures and temperatures of our experiments. Thus here, both pressure and nitrogen are required for Re and Zn to react and form the $D0_{24}$ structure, and this structure rather than the Cu_3Au structure is recovered at ambient pressure.

Insight, from the polyhedral point of view as to why the $D0_{24}$ structure is stabilized by nitrogen, is gained from stability studies on ambient pressure superlattice modifications. For example, Ti_3AlN has the antiperovskite structure.[23] However, Ti_3Al only occurs in the $D0_{19}$ modification.[31] According to previous work, the presence of nitrogen is indispensable for the stability of Ti_3Al in the cubic antiperovskite structure.[23] It was proposed that additional electron density in the octahedral void of a hypothetical nitrogen-free cubic antiperovskite Ti_3Al would be accommodated by the electronegative interstitial nitrogen placed in this position. This effect, they reported, would be manifested by a lowering of the Fermi energy leading to a reduced density of states at the Fermi level and hence a stabilization of the cubic antiperovskite modification. That indeed charge transfer from transition metal ions to interstitial nitrogen and bond formation between the two due to p-d orbital hybridization takes place has been confirmed by numerous studies.[23,32−36] Further support for the stabilizing role provided by nonmetallic atoms can be found for the case of Ti_3Sn which only occurs in the $D0_{19}$ modification. Nevertheless, the cubic antiperovskite modification can be stabilized by the addition of hydrogen in the octahedral site with Ti at its vertices. The stabilization was again found to be induced by strong Ti 3d - H 1s hybridization that lowered the total energy of the system and was reported to be the dominant bonding contribution to the formation of Ti_3SnH.[29] Further, identification of electron localization regions indicating the need for anions for structure stabilization was highlighted in one of the early applications of the electron localization function (ELF)[37] and more recently using atoms in molecules theory (AIM).[38] These considerations denote that our novel $D0_{24}$ Re_3ZnN_x structure is stabilized by the nitrogen ions situated in the cages and their bond formation due to p-d hybridization with rhenium situated on the vertices of the cages.

Atomic Packing Analysis. In terms of atomic packing, all three A_3B superlattice structures are built up using the same close-packed single layer.[16] This layer is made of alternating rows of close-packed B atoms and an ordered close-packed row of A and B atoms such that the A atoms form triangles. These layers are then stacked on top of each other displaced laterally by some distance from an identical layer below. The three superlattice structures differ only by the repeat distance, that is, how many layers are stacked before a layer is positioned again with no lateral shift with respect to the initial one. The simplest is the hexagonal $P6_3/mmc$ $D0_{19}$ modification where the layers fall on top of each other every second layer (giving a repeat sequence ababab ...). In the cubic antiperovskite modification, the layers fall on top of each other every third layer (abcabcabc ...), and in the present $D0_{24}$ structure, the layers fall on top of each other every fourth layer (in the sequence abacabacabac ...). Thus, if the distance between the layers in the *c*-direction is given as *d*, then $D0_{19}$ has $c = 2d$, the cubic modification has $c = 3d$ and our $D0_{24}$ modification has $c = 4d$, i.e., a simple cell doubling of the structurally intimate $D0_{19}$ relative. This doubling of the unit cell in the *c*-axis, while not affecting the [001] zone axis pattern, will give rise to extra spots in other zones such as the [211] zone shown here (Figure 2c,d). From all the known longer period stacking sequences, only the $D0_{19}$ and $D0_{24}$ structures have hexagonal symmetry;[12] the others are rhombohedral or cubic which are characterized by different intensity distributions of their spots in the basal planes than those measured here. Further, higher order varieties would reveal pronounced splittings at various tilt angles excluding them from consideration here.[14] The cubic modification itself does not exhibit extra spots as present in the [211] zone, and its simulated diffraction profile as a function of tilt angle is very different from that of the hexagonal $D0_{19}$ and $D0_{24}$ modifications.[14] In all three of these modifications the A atoms, in addition to being coordinated to six B atoms in the same layer, also have three B atom neighbors in the layer just above and three in the layer just below. Indeed, the superlattice structures differ from random solid solutions by the fact that the two types of atoms order so that each type maximizes the number of atoms of the other type surrounding it.[16] This leads to two types of site, where one type of atom occupies the lattice positions only and the other, the superlattice positions only. Larger differences in electronegativity between A and B likely stabilize superlattices since this difference would induce unlike atoms to want to be closer to each other.

Thus from the atomic packing point of view, the hexagonal superlattice $D0_{19}$ and $D0_{24}$ structures fall into a somewhat odd category. They are not, strictly speaking, examples of solid solutions because the atoms are not, in the ideal $D0_{19}$ and $D0_{24}$ structures, ordered randomly on the same crystallographic site. On the other hand, they are not far from it. In these structures, the A atoms retain the lattice positions and the B atoms take up superlattice positions to have only B atoms surrounding the A atoms. But the transition between these two states could be continuous with the ordering between the two positions varied. Processing conditions can result in a range of atomic arrangements between the ideal superlattice structure and the random solution where all sites are equivalent. This has led superlattices to be regarded either as extensions of solid solutions or as intermediate phases between solid solutions and bonafide intermetallic compounds.[16] Mg−Cd for example can form both solid solutions and A_3B superlattice structures, and Ti−Ni can form both A_3B superlattice structures and intermetallic alloys.[11] Re−Zn shows no reaction up to 20 GPa after heating. It is thus not unreasonable to examine first how compatible Re and Zn are with the four Hume−Rothery criteria for solid solution formation up to 20 GPa. These guidelines for solid solution formation between A and B are radii of the two being within 15% of each other, the two having the same valency, same crystal structure, and comparable electronegativities.[16] Ambient

(31) Hong, T.; Watson-Yang, T. J.; Guo, X. Q.; Freeman, A. J.; Oguchi, T. *Phys. Rev. B* **1991**, *43*, 1940–1947.
(32) Sanjines, R.; Wiemer, C.; Hones, P.; Levy, F. *J. Appl. Phys.* **1997**, *83*, 1396–1402.
(33) Skala, L.; Capkova, P. *J. Phys.: Condens. Matter* **1990**, *2*, 8293–8301.
(34) Stampfl, C.; Mannstadt, W.; Asahi, R.; Freeman, A. J. *Phys. Rev. B* **2001**, *63*, 155106–155116.
(35) Sifkovits, M.; Smolinksi, H.; Hellwig, S.; Weber, W. *J. Magn. Magn. Mater.* **1999**, *204*, 191–198.
(36) Alling, B.; Ruban, A. V.; Karimi, A.; Peil, O. E.; Simak, S. I.; Hultman, L.; Abrikosov, I. A. *Phys. Rev. B* **2007**, *75*, 045123–045135.
(37) Savin, A.; Nesper, R.; Wengert, S.; Fassler, T. F. *Angew. Chem., Int. Ed.* **1997**, *36*, 1808–1832.
(38) Vegas, A.; Santamaria-Perez, D.; Marques, M.; Florez, M.; Baonza Garcia, V.; Recio, J. M. *Acta Crystallogr., Sect. B: Struct. Crystallogr. Cryst. Chem.* **2006**, *B62*, 220–227.

Re and Zn have metallic radii within 2.6% of each other, they have the same crystal structure ($P6_3/mmc$), but their electronegativities differ by about 15% and their conventional most stable valencies are +6 or +7 and +2, respectively.[39,40] In addition to this, we point at the anomalously large for an hcp metal c/a ratio (1.87) for Zn at ambient pressure, attributed to a lowering of band structure energy through lattice distortion, which may bear on solid solution formation. However, while the anomalous c/a ratio of Zn, at and above 20 GPa, becomes typical of hexagonal structures (1.68), and the atomic radii of Re and Zn are within 4% at 20 GPa, and both Re and Zn retain the $P6_3/mmc$ structure,[8,9,41−44] the elements still do not react. This is the case, even though their melting points are also converging to within a factor of about 2 of each other at 20 GPa, rather than 7 at ambient pressure.[44] Thus, Re−Zn solid solutions at ambient and at high pressure may not form because of the differences in their electronegativity and their valency. The noticeable difference in electronegativity is one factor that may push the system in the direction of superlattice formation. This, as discussed above, is because increased differences in electronegativity make it more favorable for atoms to strive to be surrounded by unlike atoms, which is an important factor promoting superlattice rather than solid solution formation.[16] Indeed this scenario is in many respects favorable for superlattice formation in the Re−Zn system. That is, if size ratios were too different, then with the pronounced lattice distortions, the solvent (A) would not have been able to incorporate enough solute (B) to form a superlattice in the first place. On the other hand, with the size ratios being very compatible (as they are for Re and Zn), accommodation of solute is less of an issue and electronic differences (electronegativity, valency) are handled by superlattice formation.[16] We bear in mind that electronegativity and valency values are nominal, and zinc in alloys, for example, has also been assigned a valency of zero.[16] Indeed, from the atomic packing point of view, nitrogen through electron transfer and change in the number of valence electrons may adjust the effective valency of the metallic elements[45] to a nominal configuration, making superlattice formation favorable. Pressure can also assist in shifting the balance in favor of the $D0_{24}$ superlattice structure because the $D0_{24}$ structure is only 1.2% less dense than the stoichiometric component Re and Zn at ambient conditions.

Conclusions

In this work we have recovered a hexagonal Re_3ZnN_x nitride phase that is stabilized by the combined influence of pressure and nitrogen. This adds a new dimension to the novel nitride landscape prepared under extreme conditions of pressure and temperature. In particular a $D0_{24}$-based nitride has not been observed before. On the other hand binary A_3B $D0_{24}$ and related $D0_{19}$ superlattice alloys exist in abundance. Since nitrogen is situated interstitially, it is actually not altering the backbone Re_3Zn $D0_{24}$ structure by creating, for example, new polyhedra[46] but literally making the reaction between Re and Zn possible and hence stabilizing the $D0_{24}$ structure. This then demonstrates another property of nitrogen in conjunction with pressure, which opens up further possibilities for engineering new materials. Even when the formidable pressure variable does not alone lead to novel architectures and chemistry, addition of a small amount of nitrogen can make the new structures possible. Further, it will be very interesting to refine, using ab initio calculations, how the changes in the electronic structure of Zn, with the normalization of its c/a ratio upon compression, make it more compatible with Re, requiring now, at 20 GPa, just an injection of nitrogen to promote alloying between the two. Finally, this methodology can be used with other ions as well, including hydrogen, deuterium, carbon, or oxygen, altogether thus markedly enhancing our options for making targeted, normally unformable new materials and simultaneously augmenting the application domain further, for example, to hydrogen storage.

Methods

The reactants were Re powder (325 mesh, 99.99% Alfa Aesar), Zn powder (100 mesh, 99.9%, Alfa Aesar), and Zn_3N_2 powder (99% Alfa Aesar). For the ambient pressure experiments, samples were heated in a tube furnace with a gas mix of 90% argon/10% hydrogen flowing through. Four experiments were performed at ambient pressure, two with mixtures of 33 mol %:66 mol % Re:Zn and two with mixtures of 33 mol %:66 mol % Re:Zn_3N_2. These were placed in boron nitride capsules and heated to 920 K within 10 min. The samples were held there for 5 min and cooled to room temperature within 20 min. For the high pressure experiment at 5 GPa, an approximate mixture of 33 mol %:66 mol % Re:Zn_3N_2, was loaded in a capsule made of 0.025 μm thick rhenium foil. The target pressure of 5 GPa was reached after 2 h. The target temperature of 1500 K was attained in 20 min. The sample was held there for 2 min and quenched within minutes. Three high pressure experiments at 20 GPa were performed with approximate mixtures of 33 at%:66 at% Re:Zn, Re:Zn_3N_2, and pure Zn_3N_2 powders loaded in capsules made of 0.025 μm thick rhenium foil. The target pressure of 20 GPa was reached after 4 h. The target temperatures of either 1800 or 1900 K were attained in 20 min. The 33 at%:66 at% Re:Zn and Re:Zn_3N_2 mixtures were held at the target temperature for 2 min and cooled to room temperature with a cooling rate of 40 K/min within about 50 min, and the Zn_3N_2 experiment was quenched within minutes. The samples from both the ambient and high pressure experiments were recovered and polished for electron microscopy measurements. The two experiments with Zn_3N_2 at 20 GPa both gave rise to the Re_3ZnN_x phase whereas all the other six experiments gave no reaction between Re and Zn. Description in great detail of the procedures used for both the high pressure measurements and the processing procedures after recovery are described elsewhere.[47] High pressures and temperatures were applied using a multinanvil apparatus (Hymag, 1000 ton hydraulic press and a $LaCrO_3$ heater). The recovered samples were carbon coated for scanning electron microscopy (SEM) (Philips XL30CP, with an energy dispersive X-ray analyzer [Oxford instruments EDX detector - SiLi crystal with PGT spirit analysis software]) for chemical analysis. The acceleration voltages used were 10 kV and 20 kV in backscattering electron mode (BSE) for chemical contrast. The lower voltage served to enhance detection of the nitrogen light element by reducing the effect of X-ray absorption.[48] Samples were also investigated with a Philips CM30,

(39) Fletcher, D. A.; McMeeking, R. F.; Parkin, D. *J. Chem. Inf. Comput. Sci.* **1996**, *36*, 746–749.
(40) Varga, T. K.; Bello, C. PermaCharts: Periodic Table of the Elements, Cheektowaga, NY, 2002.
(41) Schulte, O.; Holzapfel, W. B. *Phys. Rev. B* **1996**, *53*, 569–580.
(42) Steinle-Neumann, G.; Stixrude, L. *Phys. Rev. B* **2001**, *63*, 054103−054108.
(43) Duffy, T. S.; Shen, G.; Heinz, D. L.; Shu, J.; Ma, Y.; Mao, H. K.; Hemley, R. J.; Singh, A. K. *Phys. Rev. B* **1999**, *60*, 15063–15073.
(44) Young, D. A. *Phase Diagrams of the Elements*, 1st ed.; University of California Press: Berkeley, 1991.
(45) Brewer, L. *Science* **1968**, *161*, 115–122.
(46) Xia, S.; Bobev, S. *J. Alloys Compd.* **2007**, *427*, 67–72.
(47) Guillaume, C.; Morniroli, J. P.; Frost, D. J.; Serghiou, G. *J. Phys.: Condens. Matter* **2006**, *18*, 8651–8660.
(48) Goldstein, J. I.; Newbury, D. E.; Patrick, E.; Joy, D. C.; Romig, A. D.; Lyman, C. E.; Fioru, C.; Lifshin, E. *Scanning Electron Microscopy and X-ray Microanalysis*, 2nd ed.; Plenum Press: New York, 1992.

transmission electron microscope (TEM), equipped with a Gatan slow scan CCD camera and with Digital Micrograph software for acquisition of electron diffraction patterns and bright-field imaging. Particles of the reaction product from the polished half capsule were taken under an 126× total magnification optical microscope, using a sharp tungsten carbide needle and dispersed onto the thin carbon film of a labeled 3 mm diameter copper grid (Agar scientific). Electron diffraction and bright-field images were obtained using 300 kV acceleration voltage. A 440 mm camera length was used for recording electron diffraction patterns. Both selected-area electron diffraction and convergent beam and microdiffraction (electron diffraction with a nearly parallel incident beam focused on the specimen with a small spot-size in the range 10 to 50 nm) were used for collecting diffraction patterns.[49,50] All the zone-axis diffraction patterns collected were interpreted using the software "Electron Diffraction" versions 6.8 and 7.01.[14,15]

Acknowledgment. High-pressure experiments were performed at the Bayerisches Geoinstitut under the EU "Research Infrastructures: Transnational Access" Programme (Contract No. 505320 (RITA) - High Pressure). We also acknowledge the use of the EPSRC Chemical Database Service at Daresbury and the generous assistance of R. A. Meeking. We further thank N. Odling for many discussions. We also thank N. Cayzer, J. Craven, and E. Passmore for much assistance with scanning microscopy, M. Hall for the demanding solids processing, and L. Nigay for critical readings of the manuscript.

JA903976J

(49) Morniroli, J. P.; No, M. L.; Rodriguez, P. P.; San Juan, J.; Jezierska, E.; Michel, N.; Poulat, S.; Priester, L. *Ultramicroscopy* **2003**, *98*, 9–26.

(50) Holmestad, R.; Morniroli, J. P.; Zuo, J. M.; Spence, J. C. H.; Avilov, A. *Electron Microsc.* **1997**, *153*, 137–140.